The Application of Risk Minimization to the Selection of Fiber Optic Sensors for an Aerospace Structural Monitoring Application

ADRIELLY HOKAMA RAZZINI, MICHAEL D. TODD,
IDDO KRESSEL, YOAV OFIR and MOSHE TUR

ABSTRACT

This work proposes an optimal fiber optic sensor placement framework for structural health monitoring (SHM) applications. The framework is applied to an aircraft's wing spar entirely made of composite materials. The damage of interest is debonding between laminates, which may cause local buckling that results in reduced structural load carrying capabilities. A high-fidelity finite element (FE) model is used as a synthetic data generator. The inputs to the model are loads and debonding damage parameters (size and location), and the outputs are uniaxial strain measurements and buckling eigenvalues. "Run time" surrogate models are created using different machine learning methods to overcome the high computational costs of each run of the physics-based model. Then, Bayesian inference is used to estimate the damage parameters given strain measured at candidate sensor locations. These estimations are used to assess damage criticality, which is linked to buckling eigenvalues, and transformed into decisions. Bayesian optimization is used to select the candidates that minimize a utility function that considers the costs associated with making a certain decision plus the costs of acquiring and installing the SHM hardware (sensors, data acquisition system, etc.). The candidate with the lowest cost is selected. The resulting optimal sensor configuration is presented, consisting of the number of sensors to be deployed and their respective locations. The importance of defining an objective function that reflects the goal of the SHM system (e.g., maximizing the probability of detection, minimizing the probability of false alarms, or a balance of both) are also discussed.

Adrielly Hokama Razzini, Department of Structural Engineering, University of California San Diego, 9500 Gilman Dr, La Jolla, CA 92093, USA
Michael D. Todd, Department of Structural Engineering, University of California San Diego, 9500 Gilman Dr, La Jolla, CA 92093, USA
Iddo Kressel, Engineering Division, Israel Aerospace Industries (IAI), Ben Gurion International Airport, Israel
Yoav Ofir, Engineering Division, Israel Aerospace Industries (IAI), Ben Gurion International Airport, Israel
Moshe Tur, School of Electrical Engineering, Tel-Aviv University, Tel-Aviv, Israel

INTRODUCTION

One of the primary purposes of implementing a structural health monitoring (SHM) system is to enable real-time monitoring of a structure, allowing for continuous assessment of its condition. This assessment helps in making informed decisions regarding the present and future capability of the system to operate safely and reliably [1]. However, the success of an SHM system is directly related to the quality of the data being collected and the features extracted from them [2]. Optimal sensor placement (OSP) strategies work to maximize the ability to collect and discriminate relevant data features given all imposed constraints [3, 4].

In aerospace applications—where weight is a critical factor—the number of sensors, data acquisition systems and power supplies available is limited. Structural inaccessibility and the costs of acquiring, installing, and maintaining the hardware must also be considered [5]. This paper presents an OSP framework that considers these constraints and minimizes the costs associated with the system and its decisions, where false positives and false negatives are penalized.

This work considers arrays of fiber Bragg gratings (FBGs) used as the sensing mechanism. These sensors are lightweight and compact, can be embedded within composite materials [6], are immune to electromagnetic interference, and have high resolution and sensitivity to strain measurements, making them suitable for aerospace applications. The steps of the framework and results will be discussed in the following sessions.

THE OPTIMAL SENSOR PLACEMENT FRAMEWORK

Step 1 – Defining the Structure and Damage of Interest

The structure of interest is a wing spar. The spar is the main structural component of an aircraft wing, and it extends from the wing root to the wingtip. In this work, the spar is 5m long, shaped as an I-beam entirely made of carbon fiber reinforced polymer composites, with a sandwich panel web. Images of the finite element (FE) model of the structure are shown in Figure 1, and more details about the model can be found in [7].

The damage of interest is debonding between the top cap and the web, which may be caused by manufacturing imperfections or introduced during service. When the top cap is under compression, this debonding damage may cause local buckling, preventing the aircraft from carrying its ultimate service load. If this occurs, the damage is considered critical to the structure. This behavior was simulated in a finite element analysis, and it is governed by the buckling eigenvalue, λ. Given that

$$F_{failure} = \lambda \times F_{applied} \tag{1}$$

where F are the loads, any damage condition that makes $\lambda < 1$ for the applied loads are considered critical. This is the fundamental damage limit state.

The debonding damage was fully characterized by a set of parameters $\theta = \{\sigma, x\}$. These two random variables are the damage size, σ, and location along the beam, x. Thus, the damage was probabilistically characterized by the joint probability density function $p(\sigma, x)$.

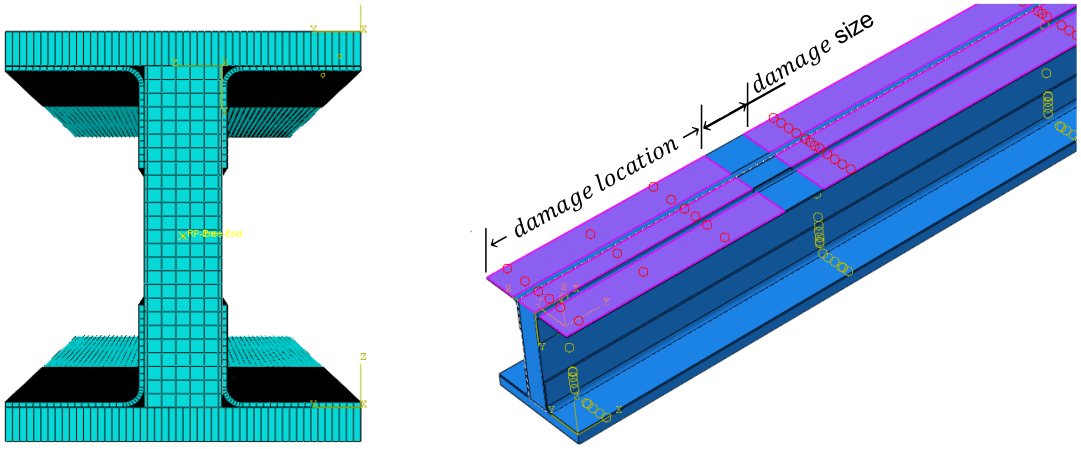

Figure 1. Left: cross-section view and FE model's mesh of the spar. Right: representation of debonding damage by removal of tie constraints, shown in purple (top flange removed from the image) [7].

Although stress concentrations from the loading profile might induce some correlation between damage size and location, it is reasonable to assume that they are independent parameters. Then, the joint density of the damage parameters was factored as $p(\sigma, x) = p(\sigma)p(x)$. These were the prior distributions of the damage parameters.

Step 2 – Data acquisition and/or synthetic data generation

The second step of the framework is acquiring data from the structure, under different environmental, operational, and damage conditions. In many cases, these data can be almost impossible to acquire, especially if damage is irreversible. In this work, the lack of directly available field data was mitigated using a detailed finite element model [7], as shown in Figure 1. A forward model can be written as in Equation (2)

$$\varepsilon = h(F, \sigma, x) + w \tag{2}$$

where ε is the output strain (at any location), and $h(*)$ is the finite element model with probabilistic inputs of load state F and damage state characterized by σ and x. Gaussian white noise, w, with $\mu_w = 0 \; and \; \sigma^2 = s_w$ can be added to the strain obtained from the finite element model, modeling the uncertainty measured in the strain data.

Since $h(*)$ is quite complex, forward simulation to map inputs to measurements can be achieved by running the finite element model sampling across all the probabilistic variables, F, σ, x, and adding noise, w. However, because criticality (failure) is not determined by the presence of the debonding damage, but rather by their effect on local buckling, two runs per probabilistic input are necessary: one normal application of Equation (2) to obtain strain, followed by a buckling analysis to get the buckling eigenvalue, λ. Therefore, the buckling step can be written as

$$\lambda = b(h(F, \sigma, x) \tag{3}$$

where $b(*)$ is the buckling analysis operator applied to the finite element model, h.

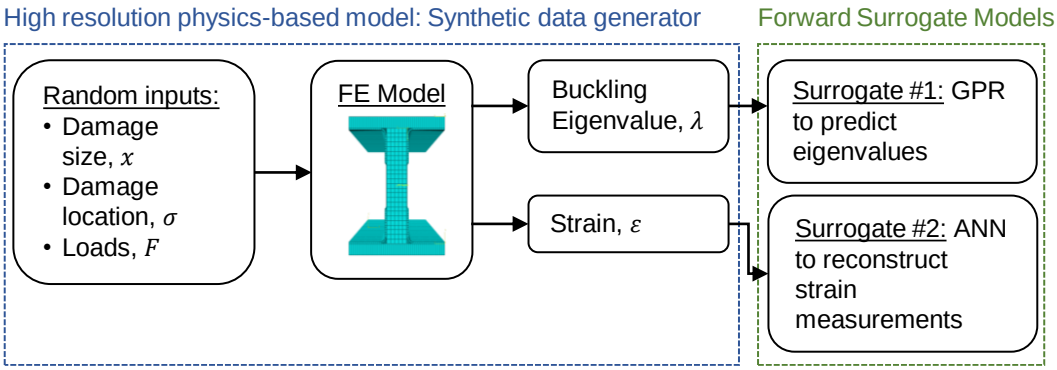

Figure 2. Data generation step using a high-resolution physics-based finite element model [7] and forward surrogate models [8].

From appropriate input space sampling, the distribution of ε can be obtained while finding the corresponding buckling eigenvalue for the same input conditions. However, in practice, strain is measured with discrete FBG sensors to infer whether local buckling has occurred or not. Therefore, it is necessary to obtain the probability that buckling $p(\lambda)$ has occurred, given strain measurements. Doing so requires thousands of executions of the two-step finite element model, which is very time consuming.

To overcome this challenge and to achieve enough Monte Carlo simulations with reasonable computational cost/time, two surrogate models were built in the forward direction [8]: a Gaussian process regressor (GPR) to predict eigenvalues, and an artificial neural network (ANN) to reconstruct strain measurements.

To create the surrogate models, the finite element model had to be executed enough times to create training, testing, and validation sets. Assumed prior probabilities of damage size, varying from 0.01m to 0.150 m, and damage location, from 0 to 5 m, were used to create a comprehensive database of nearly 1,000 different damage scenarios, using Latin Hypercube sampling as a space-filling technique. Manually executing such a large computational campaign would be impossible, therefore a Python script was created and integrated to ABAQUS to change the damage parameters and make all necessary model adjustments (constraints, meshes, etc.) between each run, execute the analysis, and save the results [7]. A summary of this process is shown in Figure 2.

Step 3 – Develop the damage diagnosis model

Consider strain measurements $\boldsymbol{y}$ acquired from the fiber optics sensors on the real structure, placed at a certain design $\boldsymbol{d}$, while $\boldsymbol{G}$ are strain measurements generated via surrogate model or FE model. From the forward model in Equation (2), by considering the loads, F, fixed as the maximum service load, $\boldsymbol{G}(\boldsymbol{d}, \boldsymbol{\theta})$ can be written as

$$\boldsymbol{G}(\boldsymbol{d}, \boldsymbol{\theta}) = \boldsymbol{L}(\boldsymbol{d})h(\boldsymbol{\theta}) \tag{4}$$

where $\boldsymbol{L}$ is the configuration vector, linking the measurements $\boldsymbol{y}$ to the model's strain response h. It is a Boolean vector, with either 1 or 0 values, corresponding to the measured and non-measured strain components. In other words, it is a selection operator of the measured strain, out of the complete vector h extracted from the FE model. In

addition, $\boldsymbol{L}$ depends on the spatial position of the sensors, hence $\boldsymbol{L} = \boldsymbol{L}(\boldsymbol{d})$ is a function of the design variable $\boldsymbol{d}$. Because the model's response h depends on the parameters $\boldsymbol{\theta}$, the measured strain can be generalized as:

$$\boldsymbol{y} = \boldsymbol{G}(\boldsymbol{d}, \boldsymbol{\theta}) + \boldsymbol{w} \tag{5}$$

Within the Bayesian inference theory, the probability distribution function of the damage parameters $\boldsymbol{\theta}$ is updated as the data are measured. According to the Bayes theorem [9]:

$$p(\boldsymbol{\theta}|\boldsymbol{y}, \boldsymbol{d}) = \frac{p(\boldsymbol{y}|\boldsymbol{\theta}, \boldsymbol{d})p(\boldsymbol{\theta}|\boldsymbol{d})}{p(\boldsymbol{y}|\boldsymbol{d})} \tag{6}$$

where $p(\boldsymbol{\theta}|\boldsymbol{y}, \boldsymbol{d})$ is the posterior distribution, $p(\boldsymbol{y}|\boldsymbol{\theta}, \boldsymbol{d})$ is the likelihood, $p(\boldsymbol{\theta}|\boldsymbol{d})$ is the prior distribution and $p(\boldsymbol{y}|\boldsymbol{d})$ is the evidence. Notice that the prior distribution of the damage parameters is independent of the design (sensor placement) [10], so

$$p(\boldsymbol{\theta}|\boldsymbol{d}) = p(\boldsymbol{\theta}) \tag{7}$$

According to [10], the likelihood function can be numerically estimated as

$$p(\boldsymbol{y^i}|\boldsymbol{\theta^j}, \boldsymbol{d}) = p_w[\boldsymbol{y^i} - \boldsymbol{G}(\boldsymbol{d}, \boldsymbol{\theta^j})] \tag{8}$$

This estimation is given as follows:

1. Generate N_{out} (e.g., 2,000 cases) combinations of damage size and damage locations, $\boldsymbol{\theta}^i = \{\boldsymbol{\sigma}, \boldsymbol{x}\}$, following the prior distributions of each damage parameter.
2. Generate N_{in} (e.g.,5,000 cases) combinations of damage size and damage locations $\boldsymbol{\theta}^j = \{\boldsymbol{\sigma}, \boldsymbol{x}\}$ via permutation, where $N_{out} \neq N_{in}$.
3. Use the forward model (ANN) to generate the strain measurements for each damage size and damage location from $\boldsymbol{\theta}^i$ and $\boldsymbol{\theta}^j$: h($\boldsymbol{\theta^i}$) and $\boldsymbol{h}(\boldsymbol{\theta^j})$.
4. For any sensor array $\boldsymbol{d} = \{d_1, d_2, \ldots, d_k\}$, calculate $\boldsymbol{G}(\boldsymbol{d}, \boldsymbol{\theta^j})$.
5. Finally, $p(w)$ is known, as discussed in Equation (2).

Therefore, for any given strain measured with the FBG sensors, the likelihood $p(\boldsymbol{y}|\boldsymbol{\theta}, \boldsymbol{d})$ can be estimated, and the posterior estimate of the damage parameters is given by Equation (6). Then, the estimated damage parameters $\widehat{\boldsymbol{\theta}}$, can be used as inputs to the GPR surrogate model to estimate the buckling eigenvalue. If $\lambda < 1$, the damage is considered critical to the structure, while $\lambda > 1$ means that the damage is not critical.

Step 4 – Define the cost function

Let C_{ij} be the cost of deciding that the structural state is M_i when the true state is M_j. Notice that C_{ij} only penalizes incorrect decisions (false positives and false negatives). In aerospace applications, false negatives usually have a higher cost associated with them. However, a high probability of false positives causes unnecessary

grounding of the aircraft, and the costs of unscheduled downtime can also be high. The user must define C_{ij} values that define the goal for their SHM system. The cost of decision is defined as:

$$C_{decision} = \sum_{i,j=0}^{1} C_{ij}\, P(D_i|M_j)P(M_j) \tag{9}$$

The design cost, C_{SHM}, is defined as:

$$C_{SHM} = C_{sensors} + C_{DAQ} + C_{ground\,station} + C_{installation} \tag{10}$$

The total cost, or Bayes risk, is given by:

$$\hat{C}(\boldsymbol{d}) = (C_{decision} + C_{SHM})/N \tag{11}$$

where N is a normalization factor. The Bayes risk $\hat{C}(\boldsymbol{d})$ is computed as follows:

1) Creation of a Boolean representation of the sensor placement along all possible locations: $L(\boldsymbol{d}) \in \{1,0\}$.
2) The measured strain ($\boldsymbol{y}$) is emulated by adding Gaussian white noise $\boldsymbol{w}\sim N(\boldsymbol{0}, \sigma^2\boldsymbol{I})$ to the strain $\boldsymbol{G}(\boldsymbol{d}, \boldsymbol{\theta}^i) = \boldsymbol{L}(\boldsymbol{d})\boldsymbol{h}(\boldsymbol{\theta}^i)$.
3) The likelihood $P(\boldsymbol{y}^i|\boldsymbol{\theta}^j, \boldsymbol{d})$ is numerically estimated using sequential Monte Carlo [10].
4) The likelihood is then used to estimate the maximum a posteriori probability of the damage state $\boldsymbol{\theta}^i$.
5) The GPR surrogate is used to estimate the N_{out} buckling eigenvalues, λ, associated with each damage size and damage location in the $\boldsymbol{\theta}^i$ vector.
6) The buckling eigenvalues are used to estimate damage criticality ($\lambda < 1\ is\ critical$).
7) As this is a supervised learning method, so the true damage state and its equivalent λ are known, and a confusion matrix can be generated. The performance (PFA and PoD) of the given sensor array can be estimated.
8) The costs associated with the performance and the design are calculated.

Step 5 – Perform Bayesian Optimization

The final step of the framework is to perform the Bayesian optimization. Bayesian optimization is a technique used for optimizing functions that are expensive to evaluate. It employs a probabilistic model to balance exploration and exploitation of the search space, iteratively selecting the next best point to evaluate based on the posterior distribution, efficiently searching for the optimal solution. The algorithm stops searching when it reaches the maximum number of iterations or another specified criterion.

To perform the optimization, the constraints must be defined (e.g., sensor resolution, boundaries, and distance between sensors). Then, using the damage diagnosis and cost function from the previous steps, perform *n* Bayesian optimizations for the k-th sensor in the sensor array $\boldsymbol{d} = \{d_1, d_2, \dots, d_k\}$ by minimizing the Bayes risk.

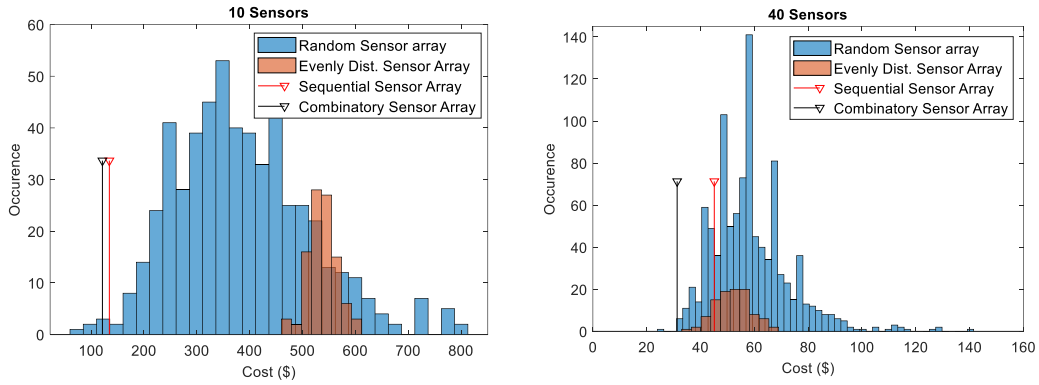

Figure 3. Results from the Bayesian optimization. Left: 10 sensors. Right: 40 sensors. Notice that the axes do not have the same limits.

RESULTS

There are two ways in which the optimized sensor array $\boldsymbol{d}$ can be obtained. The first one is sequentially, i.e., finding the sensor that offers the minimum cost and fixing it to the array, then optimizing for the second sensor considering that sensor #1 is already fixed, and so on, until the k-th sensor is fixed. The second method is named combinatory, where the algorithm optimizes for all k sensors at once.

Figure 3 shows a histogram in which the cost was evaluated for 1,000 different randomly selected sensor arrays. Then, the same damage cases were evaluated multiple times by evenly distributed sensor arrays. Finally, the damage cases were used to evaluate the cost obtained via optimization, both sequential (red) and combinatory (black). Figure 4 shows the ROC curves for the same set of sensors presented in Figure 3. It is shown that the performance of both sequential and combinatory provide similar results for 10 sensors, with a PFA around 60% and similar costs. For 40 sensors, however, the combinatory optimization performs much better, with a 12% decrease in the PFA and lower average cost. This comes at a high computational expense.

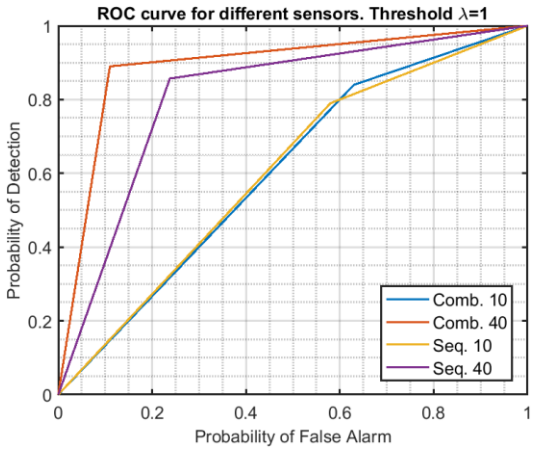

Figure 4. ROC curves for optimized sensors obtained sequentially and combinatory. The threshold is $\lambda = 1$, which is the criticality limit.

CONCLUSIONS

This paper presented the steps of an optimal sensor placement framework general enough to accommodate different structures and damage diagnosis models, given that enough data can be acquired and/or generated. It was shown that the decision cost must reflect the goal of the SHM system. In this application, for instance, false negatives were more heavily penalized than false negatives. The optimization considered the fact that not all damage can be detected with a limited amount of sensors and provided the best sensor locations that minimized false negatives while considering imposed constraints.

The need for computationally efficient surrogate models to replace the FE model became evident as thousands of samples were used to estimate the likelihood. The difference in performance between sequential and combinatory optimization was discussed – while the combinatory technique offered improved performance, it came at a cost of much higher computational expenses, as the Bayesian optimization must be executed for all k sensors at once. Finally, the damage criticality threshold was kept fixed at $\lambda = 1$. However, not all damage that provide $\lambda < 1$ offer the same level of criticality, e.g., a case that yields $\lambda = 0.5$ is almost twice as critical than a case that yields $\lambda = 0.98$. Therefore, different levels of threshold can be added to represent different levels of criticality, which might improve the performance of the system.

REFERENCES

1. Zonta, D., Glisic, B., & Adriaenssens, S. 2013. "Value of information: impact of monitoring on decision-making." *Structural Control and Health Monitoring, 21(7), 1043–1056.*
2. Farrar, C. R., & Worden, K. 2012. "Structural health monitoring: a machine learning perspective". John Wiley & Sons.
3. Flynn, E. B., & Todd, M. D. 2010. "A Bayesian approach to optimal sensor placement for structural health monitoring with application to active sensing". *Mechanical Systems and Signal Processing*, *24*(4), 891-903.
4. Ostachowicz, W., Soman, R., & Malinowski, P. 2019. "Optimization of sensor placement for structural health monitoring: A review". *Structural Health Monitoring*, *18*(3), 963-988.
5. Razzini, A.H., Todd, M.D , Kressel, I., Ofir, Y., and Tur, M. 2023. "Optimal Fiber Optic Sensor Placement Framework for Structural Health Monitoring of an Aircraft's Wing Spar". *Data Science in Engineering, Volume 10: Proceedings of the 41st IMAC, A Conference and Exposition on Structural Dynamics 2023*, pp. -
6. Kressel, I., Dorfman, B., Botsev, Y., Handelman, A., Balter, J., Pillai, A.C.R., Prasad, M.H., Gupta, N., Joseph, A.M., Sundaram, R. and Tur, M. 2015. "Flight validation of an embedded structural health monitoring system for an unmanned aerial vehicle". *Smart Materials and Structures*, *24*(7), p.075022.
7. Razzini, A.H., Todd, M.D., Kressel, I., Offir, Y., Tur, M., Yehoshua, T. 2023 "Damage Assessment of an Aircraft's Wing Spar Using Gaussian Process Regressors". In: Rizzo, P., Milazzo, A. (eds) European Workshop on Structural Health Monitoring. EWSHM 2022. *Lecture Notes in Civil Engineering*, vol 270.
8. Razzini, A.H., Kressel, I., Ofir, Y., Tur, M., Yehoshua, T. and Todd, M.D. 2022. "Development of a Surrogate Model for Structural Health Monitoring of a UAV Wing Spar". *Data Science in Engineering, Volume 9: Proceedings of the 40th IMAC, A Conference and Exposition on Structural Dynamics 2022* (p. 99).
9. Sivia, D., & Skilling, J. 2006. "Data analysis: a Bayesian tutorial". OUP Oxford.
10. Capellari, G., Chatzi, E., & Mariani, S. 2018. "Structural health monitoring sensor network optimization through Bayesian experimental design". *ASCE-ASME Journal of Risk and Uncertainty in Engineering Systems, Part A: Civil Engineering*, *4*(2), 04018016.